TRANSIENT RESPONSE ANALYSIS FOR A CIRCULAR SANDWICH PLATE WITH AN FGM CENTRAL DISK

H.-L. Dai *

State Key Laboratory of Advanced Design and Manufacturing for Vehicle Body
Hunan University
Changsha, China

Key Laboratory of Manufacture and Test Techniques for Automobile Parts
Ministry of Education
Chongqing University of Technology

Department of Engineering Mechanics
College of Mechanical & Vehicle Engineering
Hunan University
Changsha, China

T. Dai **S.-K. Cheng**

State Key Laboratory of Advanced Design and Manufacturing for Vehicle Body
Hunan University
Changsha, China

Department of Engineering Mechanics
College of Mechanical & Vehicle Engineering
Hunan University
Changsha, China

ABSTRACT

In this paper, transient response analysis of a circular sandwich plate with a functionally graded material (FGM) central disk and two piezoelectric layers is presented. Material properties of the FGM central disk for the circular sandwich plate are assumed to vary through the structural thickness according to a power law and the Poisson's ratio is assumed as the same constant. Based on the first-order shear deformation theory and geometric nonlinear relationship, the nonlinear motion equations of the circular sandwich plate are formulated by using the Hamilton's variational principle, then combining with the boundary and initial conditions, the whole problem is solved by adopting the finite difference method, Newmark method and iterative method. Numerical results are presented to illustrate that the volume fraction index, geometric parameters, mechanical and electrical loads have a great influence on transient response of the circular sandwich plate.

Keywords: Transient response, Circular sandwich plate, FGM central disk, Piezoelectric layer.

1. INTRODUCTION

FGM represents a concept of composite material of which the compositions and properties varying continuously along its thickness or length. A typical kind of FGM used as thermal insulation material is constructed with metals and ceramics through powder metallurgy processes [1,2]. The parts under high temperatures have higher content of ceramics than metals and vice versa. Mechanical properties of this material always show a smooth and continuous change from one surface to the other by varying the volume fraction of constituent materials [3-6]. FGM structures often have the ability to withstand high temperatures while keep structural integrity, but they are easy to be sensitive to large temperature gradients or mechanical loads. Investigations on various aspects of FGM structures can be found in literatures.

Based on the third-order shear deformation plate theory, Ma and Wang [7] solved the axisymmetric bending and buckling problems of FGM circular plates. Based on von Karman's plate theory, Li *et al*. [8] presented thermomechanical post-buckling of an imperfect FGM circular plate subjected to both mechanical load

* Corresponding author (hldai520@sina.com)

DOI : 10.1017/jmech.2015.7
Copyright © 2015 The Society of Theoretical and Applied Mechanics, R.O.C.
https://doi.org/10.1017/jmech.2015.7 Published online by Cambridge University Press

and transversely non-uniform temperature rise. Using the unconstrained third-order shear deformation plate theory, Saidi *et al*. [9] studied axisymmetric bending and buckling of perfect FGM circular plates. Based on the Mindlin's first-order shear deformation plate theory, an exact closed-form frequency equation was presented by Hosseini-Hashemi *et al*. [10] for free vibration analysis of circular and annular moderately thick FGM plates. Utilizing the multi-modal energy approach, Alijani *et al*. [11] investigated geometrically nonlinear vibration of FGM rectangular plates in thermal environments. Considered the geometrically nonlinear relations and temperature-dependent properties of the material, Hu and Zhang [12] investigated the bifurcation and chaos of a clamped circular FGM plate. Applying the finite difference method and Newmark scheme, Dai and Xie [13,14] studied the buckling and thermoelastic dynamic behaviors of FGM cylinders. Dai *et al*. [15] also gave a nonlinear dynamic analysis for FGM circular plates. Based on the first-order shear deformation theory, Golmakani and Kadkhodayan [16] investigated the axisymmetric bending and stretching of circular and annular functionally graded plates with variable thicknesses.

There are both elastic and electric fields in the piezoelectric material, electric charge appears when this material subjected to external mechanical deformations, while deformations occur when electric potential imposed on it. Because of these features, piezoelectric material has been widely used in various engineering applications such as sensors and actuators. Studies of piezoelectric materials are also abundant in literatures.

Zhang and Shang [17] presented an exact analysis of functionally graded piezothermoelectric rectangular plate. Much research on all aspects of FGM plates and shells had been reported. In recent several years, Li *et al*. [18] investigated the problem of a functionally graded piezoelectric material (FGPM) circular plate subjected to a uniform electric potential difference between the upper and lower surfaces. Birschetto and Carrera [19] gave a static analysis of a single-layered FGPM plate. Based on the three-dimensional theory of piezoelectricity, Wang *et al*. [20] investigated the axisymmetric bending of a circular plate whose material properties vary along the thickness. Resorting to the Fourier series expansions and state-space method, Alibeigloo [21] presented analytical solutions for the temperature, stress and displacement fields for an FGM host plate with simply supported edges under applied electrical and thermal or mechanical loads. Based on the higher-order shear plate theory and elastic piezoelectric theory, Mao *et al*. [22] investigated the creep buckling and post-buckling of the laminated FGPM plate. By employing the stress functions, a similar analysis was developed by Li *et al*. [23] for the problem of FGM plates subjected to bending and tension. Applying the Galerkin finite element method and Newmark method, Javanbakht *et al*. [24] presented an elasticity solution for a finitely long simply-supported FGM shallow and non-shallow shell panel with two piezoelectric layers under pressure and electrostatic excitation. Birman [25] gave examples of advanced applications: Plates with piezoelectric sensors and actuators and FGM plates in detail. Using the variational formulations, khorshidvand *et al*. [26] studied thermal buckling of circular plates made of functionally graded material with surface bounded piezoelectric layers. By a meshless local Petov-Galerkin method, Sladek *et al*. [27] presented a review on the analysis of the bending of FGPM circular plates.

However, as far as we know, transient response analysis of a circular sandwich plate with an FGM central disk and two piezoelectric layers cannot been found in literatures. Due to the flexible properties that can be adapted to different work environment and engineering application, therefore, investigation of the transient response of a circular sandwich plate with an FGM central disk and two piezoelectric layers is of great value and can be a reference for studies of other FGM structures with piezoelectric layers.

In this paper, the first-order shear deformation theory and geometrically nonlinear relationship are considered, and the nonlinear motion equations of the circular plate are formulated by using the Hamilton's variation principle. Combining with boundary and initial conditions, the whole problem is solved by adopting the finite difference method, Newmark method and iterative method.

2. BASIC FORMULATIONS OF THE PROBLEM

2.1 FGM Properties

Transient response analysis is considered for a circular sandwich plate with an FGM central disk and two piezoelectric layers, the investigation is most conveniently carried out by using a cylindrical coordinate system (r, θ, z) with the origin at the center of the mid-plane ($z = 0$). The r-coordinate direction is outward radially from the centre, the z-coordinate is along the thickness direction, and the θ-coordinate is directed along the circumference of the circular sandwich plate, as shown in Fig. 1.

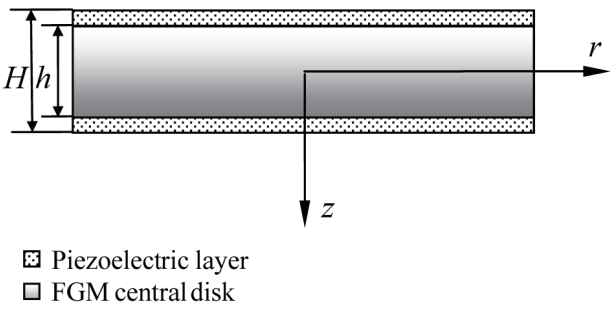


Fig. 1 Schematic of a circular sandwich plate with an FGM central disk and two piezoelectric layers.

https://doi.org/10.1017/jmech.2015.7 Published online by Cambridge University Press

The circular sandwich plate is mounted with an FGM central disk and upper and lower piezoelectric layers, an arbitrary material property P (mass density ρ and Young's modulus E) of the FGM central disk is identified as varying along the thickness of the FGM central disk and the Poisson's ratio v is assumed as the same constant. The top face ($z = h/2$) of the FGM central disk is ceramic-rich, instead, the bottom face ($z = -h/2$) is metal-rich. Meanwhile, properties of constituent materials related the function of the volume fraction can be expressed as [28,29]

$$P = P_t V_c + P_b V_m \tag{1}$$

where subscripts t and b stand for the top and bottom surfaces of the FGM central disk, respectively; V_c and V_m denotes, respectively, the ceramic and metal volume fractions and can be given by

$$V_c + V_m = 1 \tag{2}$$

where V_c is assumed as a power law function [29], and it can be denoted as

$$V_c(z) = \left(\frac{2z+h}{2h}\right)^n \tag{3}$$

where n ($0 < n < \infty$) denotes the volume fraction index, utilizing Eqs. (1) ~ (3), one gets

$$P(z) = (P_t - P_b)\left(\frac{2z+h}{2h}\right)^n + P_b \tag{4}$$

2.2 Governing Equations

Based on the first-order shear deformation plate theory, for an axisymmetric problem, the radial and transverse displacements $u(r, z, t)$ and $w(r, z, t)$ for a point on the circular sandwich plate with an FGM central disk and two piezoelectric layers are, respectively, written as

$$u_r(r, z, t) = u(r, t) + z\phi(r, t) \tag{5a}$$

$$u_z(r, z, t) = w(r, t) \tag{5b}$$

where $u(r, t)$ and $w(r, t)$ are, respectively, the radial and transverse displacements of the point on the mid-plane of the circular sandwich plate; $\phi(r, t)$ denotes the radial corner on the mid-plane of the circular sandwich plate.

Based on the above assumptions, the strains at any level z from the mid-plane are acquired by using the nonlinear strain-displacement relations as follows [30-32]

$$\varepsilon_r = \varepsilon_r^0 + zk_r\ ,\ \ \varepsilon_\theta = \varepsilon_\theta^0 + zk_\theta\ ,\ \ \gamma_{rz} = k_{rz} \tag{6}$$

where ε_r and ε_θ represent, respectively, the normal strains along the r and θ directions, γ_{rz} is the shear strain, and

$$\varepsilon_r^0 = u_{,r} + \frac{1}{2}(w_{,r})^2\ ,\ \ \varepsilon_\theta^0 = \frac{u}{r} \tag{7a}$$

$$k_r = \phi_{,r}\ ,\ \ k_\theta = \frac{\phi}{r}\ ,\ \ k_{rz} = \phi + w_{,r} \tag{7b}$$

Applying the Hooke's law, the constitutive relations of the FGM central disk for the circular sandwich plate are given as follows

$$\sigma_r^f = C_{11}^f \varepsilon_r + C_{12}^f \varepsilon_\theta \tag{8a}$$

$$\sigma_\theta^f = C_{21}^f \varepsilon_r + C_{22}^f \varepsilon_\theta \tag{8b}$$

$$\tau_{rz}^f = kC_{55}^f \gamma_{rz} \tag{8c}$$

where $C_{11}^f = C_{22}^f = E(z)/1-\nu^2$, $C_{12}^f = C_{21}^f = \nu E(z)/1-\nu^2$ and $C_{55}^f = E(z)/2(1+\nu)$, the superscript f denotes the FGM central disk of the circular sandwich plate.

The constitutive relations of the piezoelectric layer are given as follows

$$\sigma_r^p = \overline{C}_{11}^p \varepsilon_r + \overline{C}_{12}^p \varepsilon_\theta - \overline{e}_{31} E_z \tag{9a}$$

$$\sigma_\theta^p = \overline{C}_{12}^p \varepsilon_r + \overline{C}_{11}^p \varepsilon_\theta - \overline{e}_{31} E_z \tag{9b}$$

$$\tau_{rz}^p = k\overline{C}_{55}^p \gamma_{rz} + e_{15} E_r \tag{9c}$$

where $\overline{C}_{11}^p = C_{11}^p - (C_{13}^p)^2 / C_{33}^p$, $\overline{C}_{12}^p = C_{12}^p - (C_{13}^p)^2 / C_{33}^p$ and $\overline{e}_{31}^p = e_{31} - C_{13}^p e_{33} / C_{33}^p$, the superscript p denotes piezoelectric material of the circular sandwich plate.

The electric field E_i ($i = r, z$) and the electric potential ψ are related by

$$E_r = -\psi_{,r}\ ,\ \ E_z = -\psi_{,z} \tag{10}$$

where the subscript comma denotes the derivation of the latter variable.

The electric field applied is assumed to parallel the thickness direction of the piezoelectric layer. In such a way, only considering the electric component E_z along the thickness direction, if the approximate electric potential as a linear change, and the relation between electric field and voltage can be expressed as

$$E_z = \frac{2V_p}{H-h} \tag{11}$$

The units of internal force N_i ($i = r, \theta$), moment M_i ($i = r, \theta$) and shear force Q_r for the circular sandwich plate with an FGM central disk and two piezoelectric layers are, respectively, defined as

$$(N_r, N_\theta) = \int_{-h/2}^{h/2} (\sigma_r^f, \sigma_\theta^f)\, dz + \int_{h/2}^{H/2} (\sigma_r^p, \sigma_\theta^p)\, dz + \int_{-H/2}^{-h/2} (\sigma_r^p, \sigma_\theta^p)\, dz \tag{12a}$$

$$(M_r, M_\theta) = \int_{-h/2}^{h/2} (\sigma_r^f, \sigma_\theta^f)\, zdz + \int_{h/2}^{H/2} (\sigma_r^p, \sigma_\theta^p)\, zdz + \int_{-H/2}^{-h/2} (\sigma_r^p, \sigma_\theta^p)\, zdz \tag{12b}$$

https://doi.org/10.1017/jmech.2015.7 Published online by Cambridge University Press

$$(Q_r) = \int_{-h/2}^{h/2} (\tau_{rz}^f)\, dz + \int_{h/2}^{H/2} (\tau_{rz}^p)\, dz + \int_{-H/2}^{-h/2} (\tau_{rz}^p)\, dz \quad (12c)$$

where $(A_{ij}, B_{ij}, D_{ij}) = \int_{-h/2}^{h/2} C_{ij}(1, z, z^2)\, dz$, $(i = j = 1, 2, 5)$, k is the shear correction factor, and $k = 5/6$ [33,34].

Based on the Hamilton's principle, the nonlinear motion equations of the circular sandwich plate can be derived as

$$N_{r,r} + \frac{1}{r}(N_r - N_\theta) = I_1 \ddot{u} + I_2 \ddot{\phi} \quad (13a)$$

$$M_{r,r} + \frac{M_r - M_\theta}{r} - Q_r = I_2 \ddot{u} + I_3 \ddot{\phi} \quad (13b)$$

$$\left(\frac{\partial N_r}{\partial r} r + N_r\right) w_{,r} + N_r r w_{,rr} + \frac{\partial Q_r}{\partial r} r + Q_r + rq(r, t) = I_1 r \ddot{w} \quad (13c)$$

where

$$(I_1, I_2, I_3) = \int_{-h/2}^{h/2} \rho(1, z, z^2)\, dz + \int_{h/2}^{H/2} \rho(1, z, z^2)\, dz + \int_{-H/2}^{-h/2} \rho(1, z, z^2)\, dz$$

and $q(r, t)$ is a transverse mechanical load.

Substituting Eqs. (6) ~ (12) into Eq. (13), the nonlinear motion equations in the form of mid-plane displacements can be got as follows

$$\left[A_{11} + (H-h)\overline{C}_{11}^p\right]\left(u_{,rr} + w_{,r} w_{,rr} + \frac{u_{,r}}{r} + \frac{1}{2r} w_{,r} w_{,r} - \frac{u}{r^2}\right) + B_{11}\left(\phi_{,rr} + \frac{\phi_{,r}}{r} - \frac{\phi}{r^2}\right) - \left[A_{12} + (H-h)\overline{C}_{12}^p\right]\left(\frac{1}{2r} w_{,r} w_{,r}\right) = I_1 \ddot{u} + I_2 \ddot{\phi} \quad (14a)$$

$$B_{11}\left(u_{,rr} + w_{,r} w_{,rr} + \frac{u_{,r}}{r} + \frac{1}{2r} w_{,r} w_{,r} - \frac{u}{r^2}\right) + \left[D_{11} + \left(\frac{H^3 - h^3}{12}\right)\overline{C}_{11}^p\right]\left(\phi_{,rr} + \frac{\phi_{,r}}{r} - \frac{\phi}{r^2}\right) - B_{12}\left(\frac{1}{2r} w_{,r} w_{,r}\right) - k\left[A_{55} + (H-h)\overline{C}_{55}^p\right](\phi + w_{,r}) = I_2 \ddot{u} + I_3 \ddot{\phi} \quad (14b)$$

$$k\left[A_{55} + (H-h)\overline{C}_{55}^p\right](r\phi_{,r} + r w_{,rr} + \phi + w_{,r}) + \left\{\left[(A_{11} + (H-h)\overline{C}_{11}^p\right](u_{,rr} + w_{,r} w_{,rr}) + \left[A_{12} + (H-h)\overline{C}_{12}^p\right]\left(\frac{u_{,r}}{r} - \frac{u}{r^2}\right) + B_{12}\left(\frac{\phi_{,r}}{r} - \frac{\phi}{r^2}\right) + B_{11}\phi_{,rr}\right\} r w_{,r} + \left\{\left[A_{11} + (H-h)\overline{C}_{11}^p\right]\left(u_{,r} + \frac{1}{2} w_{,r} w_{,r}\right) + \left[A_{12} + (H-h)\overline{C}_{12}^p\right]\frac{u}{r} + B_{12}\frac{\phi}{r} + B_{11}\phi_{,r} + 2\int_{h/2}^{H/2} -\overline{e}_{31} E_z dz\right\}(w_{,r} + r w_{,rr}) + q(r, t)\, r - I_1 r \ddot{w} = 0 \quad (14c)$$

The boundary conditions for the clamped circular sandwich plate are expressed as

$$\phi = w = w_{,r} = u = 0 \quad (15)$$

The initial conditions for the clamped circular sandwich plate are expressed as

$$w(r, 0) = 0, \quad \frac{\partial w(r, 0)}{\partial t} = 0 \quad (16)$$

3. METHOD OF SOLUTION

Consider a circular sandwich plate with an FGM central disk and two piezoelectric layers subjected to a uniform mechanical load on the top surface

$$q = q(t) \quad (17)$$

In the following discussion, the $q(t)$ is set as two cases as: (1) $q(t) = q_0 H(t)$, (2) $q(t) = q_0 \sin t$. In the first case, $H(t)$ stands for the Heaviside function, and q_0 is a constant load; in the second case, the load is considered as a simple harmonic excitation.

In order to seek an approximate solution of the nonlinear motion equations, which meet boundary conditions, using the finite difference method and the Newmark method, the unknown variable functions are discretized in space domain and in time domain, and the whole problem is solved by the iterative method synthetically.

The displacement functions u, w and ϕ are discretized in space domain and in time domain. The finite difference method is used for the space domain. The time t is equally divided into small time segments Δt, and the solution to these equations can be obtained by the iterative method, at each iterative step J, the nonlinear terms of the equations and boundary conditions are linearized and written as follows

$$(x \cdot y)_J = (x)_J \cdot (y)_{J_P} \quad (18)$$

where $(y)_{Jp}$ is the average value of that acquired in the preceding two iterations. For the initial iteration, the quadratic extrapolation method can be used to obtain it, *i.e.*

$$(y)_{J_P} = A(y)_{J-1} + B(y)_{J-2} + C(y)_{J-3} \quad (19)$$

Meanwhile, for different steps of iteration, the coefficients of A, B and C can be expressed as follows [37]

$$\begin{aligned} &J = 1: \ A = 1, \ B = 0, \ C = 0 \\ &J = 2: \ A = 2, \ B = -1, \ C = 0 \\ &J \geq 3: \ A = 3, \ B = -3, \ C = 1 \end{aligned} \quad (20)$$

Then, the inertia in Eq. (14) can be expressed as follows by using the Newmark scheme [37]

https://doi.org/10.1017/jmech.2015.7 Published online by Cambridge University Press

$$(W_{,t})_j = \Delta t\left(\varsigma(W_{,tt})_j + (1-\varsigma)(W_{,tt})_{j-1}\right) + (W_{,t})_{j-1} \tag{21a}$$

$$(W)_j = (W)_{j-1} + \Delta t(W_{,t})_{j-1} + \left(\xi(W_{,tt})_j + \left(\frac{1}{2}-\xi\right)(W_{,tt})_{j-1}\right)(\Delta t)^2 \tag{21b}$$

$$(W_{,tt})_j = \frac{\left((W)_j - (W)_{j-1}\right)}{\xi(\Delta t)^2} - \frac{(W_{,t})_{j-1}}{\xi(\Delta t)} - \left(\frac{1}{2\xi}-1\right)(W_{,tt})_{j-1} \tag{21c}$$

where the numerical values of ς and ξ depend on the integral accuracy and stability of the circular sandwich plate. Moreover, when $\varsigma = 1/2$ and $\xi = 1/4$, it is the average acceleration method.

After the above treatment, the preceding nonlinear partial differential equations are turned into a set of linear algebraic equations. For each step of iteration, the iterations lasts until the difference of the present value and the former is smaller than 10^{-5}. When the convergent solution is got, the iterative step will be terminated and then calculate the $j + 1$ step.

4. NUMERICAL RESULTS AND DISCUSSION

Example 1. To ensure the validity and accuracy of the present method, the present model is degenerated into a clamped FGM circular plate under a uniform transverse loading, which is the same as in reference [35]. w_0 represents the center deflection of the circular sandwich plate, $\bar{w} = 64w_0 D_0 / q \times a^4$ denotes the dimensionless deflection of the FGM circular plate, and the same material parameters are taken as [34]

$$\begin{aligned} &\nu = 0.288, \quad E_c = 200\text{GPa}, \\ &E_r = E_m / E_c = 0.396, \\ &D_0 = \frac{E_c \times h^3}{12 \times (1-\nu^2)} \end{aligned} \tag{22}$$

It can be observed from the Table 1 that the present results are relatively close to those of reference [35], and it can be concluded that the present numerical method is proved to be correct and reliable. In this table, FST is short for the first-order shear deformation plate theory of Mindlin, TST means the third-order shear deformation plate theory of Reddy, and FOST represents the fourth-order shear deformation plate theory. Data in this table are dimensionless.

Example 2. Considering a clamped circular sandwich plate with an FGM central disk and two piezoelectric layers subjected to mechanical excitation $q(t) = q_0H(t)$. The midpoint dimensionless deflection $W_0 = w_0 / H$ is introduced into the following investigation. The FGM central disk is composed of Zirconia-Aluminum [36] and the piezoelectric layer is taken as PZT-4A, its material parameters are selected as

Table 1 Comparison of the Dimensionless Mid-Point Deflection for the Circular FGM Plate.

n		The ratio of thickness and radius h / a					
		0.05	0.1	0.2	0.25	0.3	0.33
0	FST [33]	2.5253	2.6388	2.9792	3.2346	3.5467	3.7612
	TST [33]	2.5253	2.6375	2.9687	3.2139	3.5110	3.7137
	FOST [33]	2.5253	2.6375	2.9687	3.2139	3.5110	3.7137
	This paper	2.3921	2.6326	2.9774	3.2332	3.5455	3.7601
0.05	FST [33]	1.7013	1.7766	2.0023	2.1716	2.3785	2.5207
	TST [33]	1.7014	1.7770	2.0003	2.1655	2.3656	2.5020
	FOST [33]	1.7014	1.7771	2.0007	2.1662	2.3664	2.5031
	This paper	1.8904	1.8076	1.9288	2.4904	2.3420	2.4907
2	FST [33]	1.3882	1.4445	1.6133	1.7400	1.8947	2.0010
	TST [33]	1.3882	1.4426	1.6032	1.7222	1.8663	1.9646
	FOST [33]	1.3882	1.4426	1.6033	1.7224	1.8666	1.9650
	This paper	1.3283	1.4314	1.6092	1.7369	1.8922	1.9987
5	FST [33]	1.2343	1.2843	1.4342	1.5466	1.6841	1.7785
	TST [33]	1.2343	1.2821	1.4235	1.5283	1.6553	1.7420
	FOST [33]	1.2343	1.2822	1.4237	1.5286	1.6557	1.7424
	This paper	1.1856	1.2726	1.4305	1.5439	1.6818	1.7764

Zirconia: $E_c = 380\text{GPa}$, $\rho_c = 3800\text{kg/m}^3$,

Aluminum: $E_m = 70\text{GPa}$, $\rho_m = 2700\text{kg/m}^3$,

PZT-4A:

$C_{11} = 132\text{GPa}$, $C_{12} = 71\text{GPa}$, $C_{13} = 73\text{GPa}$,

$C_{33} = 115\text{GPa}$, $C_{55} = 26\text{GPa}$, $e_{15} = 10.5\text{C/m}^2$,

$e_{31} = -4.1\text{C/m}^2$, $e_{33} = 14.1\text{C/m}^2$, $\rho = 7500\text{kg/m}^3$.

Considering the mechanical loads are set as q_0 = 25MPa, 50MPa and the electrical closed-circuit, the comparison of the linear and nonlinear deflection distribution for the circular sandwich plate is presented in Fig. 2, where $a = 0.5\text{m}$, $h = 0.05\text{m}$, $H = 0.06\text{m}$ and $q(t) = q_0H(t)$ $(t \to +\infty)$. From Fig. 2, it can be seen that, when the mechanical load q_0 is small, the amplitude or frequency in the linear and nonlinear conditions are close. However, as the increase of q_0, large differences on both the amplitude and the frequency occur between the linear and nonlinear conditions. Hence, when the mechanical load is not small, it is far from accuracy if only linearity is considered, that is, considering the nonlinearity is necessary.

Example 3. Considering a clamped circular sandwich plate with an FGM central disk and two piezoelectric layers subjected to a mechanical excitation $q(t) = q_0 \sin t$, other conditions are the same as example 2.

https://doi.org/10.1017/jmech.2015.7 Published online by Cambridge University Press

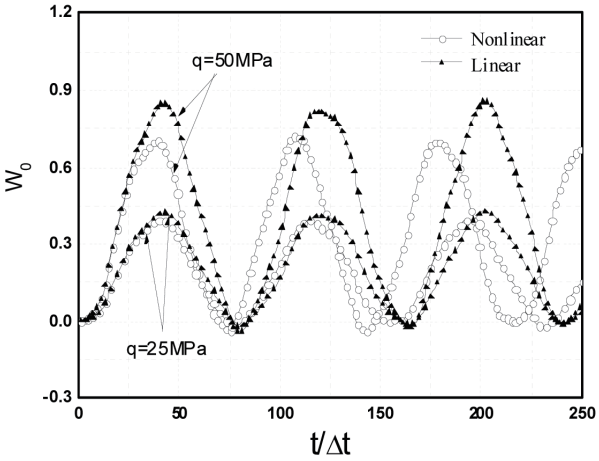


Fig. 2 Comparison of linear and nonlinear deflection distributions of the midpoint for the clamped circular sandwich plate with an FGM central disk and two piezoelectric layers under different mechanical loads.

Figure 3 shows deflection distribution of the midpoint for the clamped circular sandwich plate with different volume fraction indexes n. From Fig. 3, it can be observed that the amplitude of deflection for the circular sandwich plate increases as the volume fraction index n increases, its change is very small when the volume fraction index n arrives at a certain value, and the frequency of the deflection is the same with different volume fraction indexes n.

Figures 4 and 5 show, respectively, the distributions of the radial and hoop stresses for the circular sandwich plate with different volume fraction indexes n, where $z = 0$ and $r = 1/2a$. From two figures, it is obvious that the radial stress and hoop stress present a similar harmonic rule as the time increases. Meanwhile, the amplitudes of the radial and hoop stresses are different in the positive and negative directions, and it is bigger in the positive direction, this is because the geometric mid-plane is not the physical mid-plane of the circular sandwich plate. It is also seen from two figures that the amplitudes of the radial and hoop stresses decrease as the volume fraction index n increases, and the gap between geometric mid-plane and physical mid-plane is smaller gradually, so the amplitudes of the radial and hoop stresses decrease.

Figure 6 depicts the influence of the thickness of the piezoelectric layer for the circular sandwich plate on the amplitude of the midpoint deflection for the circular sandwich plate. From Fig. 6, it can be found that the amplitude of the midpoint deflection for the circular sandwich plate increases as the H/h decreases, which it is due to the bending stiffness of the circular sandwich plate increases at the same total thickness H as the thickness of the piezoelectric layer increases.

Figure 7 presents the influence of the ratio of thickness to radius on the deflection distribution of the circular sandwich plate with an FGM central disk and two piezoelectric layers. It is seen from the Fig. 7 that the magnitude of the midpoint deflection for the circular sandwich plate increases as the h/a decreases.

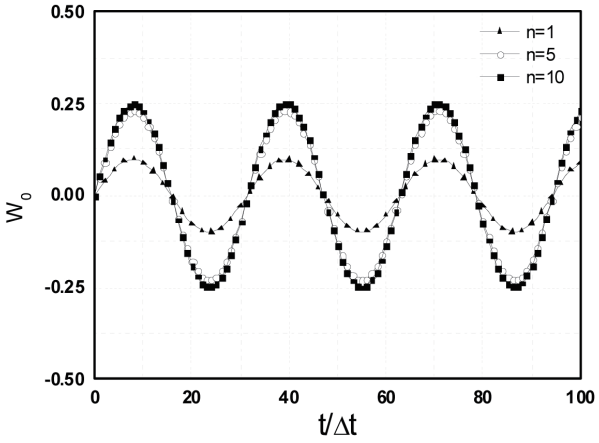


Fig. 3 The influence of the volume fraction index n on the deflection distributions of midpoint for the clamped circular sandwich plate with an FGM central disk and two piezoelectric layers.

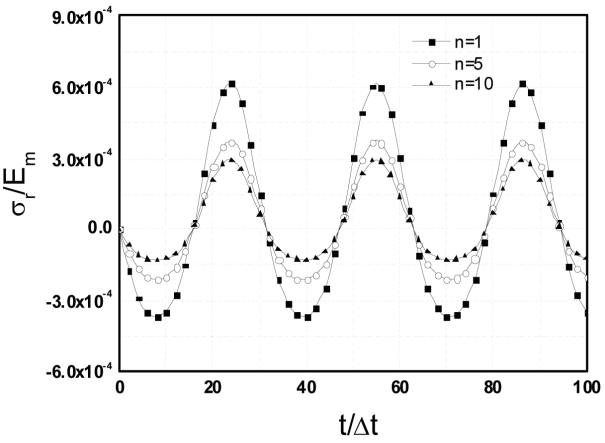


Fig. 4 The influence of the volume fraction index n on the radial stress distributions for the clamped circular sandwich plate with an FGM central disk and two piezoelectric layers and $r = 1/2a$.

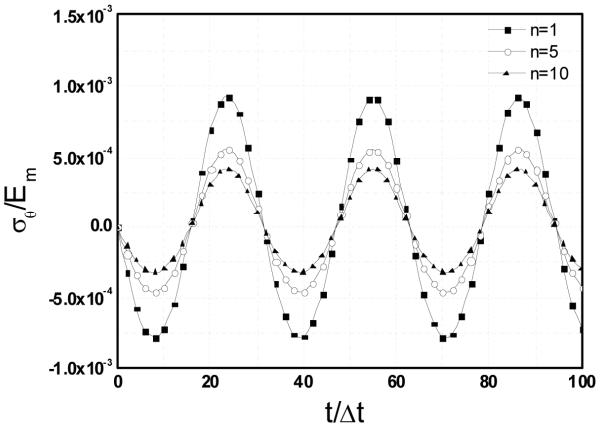


Fig. 5 The influence of the volume fraction index n on the hoop stress distributions for the clamped circular sandwich plate with an FGM central disk and two piezoelectric layers at $z = 0$ and $r = 1/2a$.

https://doi.org/10.1017/jmech.2015.7 Published online by Cambridge University Press

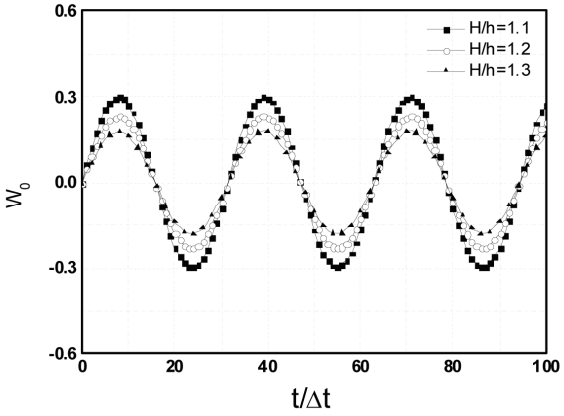


Fig. 6 The influence of the thickness of the piezoelectric layer on the reflection distributions of the midpoint for the clamped circular sandwich plate with an FGM central disk and two piezoelectric layers.

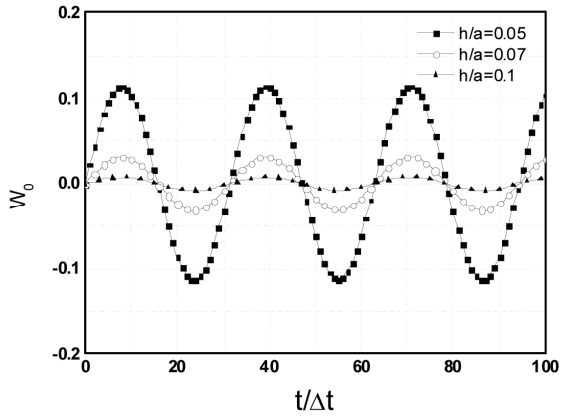


Fig. 7 The influence of the ratio of thickness to radius on the reflection distributions of the midpoint for the clamped circular sandwich plate with an FGM central disk and two piezoelectric layers.

Figure 8 shows the influence of mechanical load on the deflection distribution of the circular sandwich plate. From Fig. 8, it is found that the amplitude of the midpoint deflection for the circular sandwich plate increases as the mechanical load increases. From Figs. 6 ~ 8, one finds, the frequency of the deflection distribution for the clamped circular sandwich plate is not influenced by the geometric size of the structure and applying the mechanical excitation.

Figures 9 ~ 11 gives, respectively, the influence of electric excitation on the defection distribution, radial and hoop stresses for the clamped circular sandwich plate with an FGM central disk and two piezoelectric layers. In three figures, the maximum voltage 1000 volts are applied to piezoelectric layers of the clamped circular sandwich plate [38].

From Fig. 9, it can be noticed that the amplitude of the midpoint deflection of the circular sandwich plate decreases as the electric excitation increases, and the frequency of the deflection is identical. For deep understanding, it is effective to reduce the amplitude of

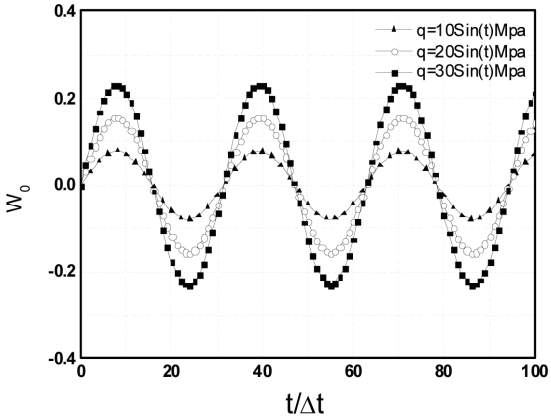


Fig. 8 The influence of the mechanical loads on the deflection distributions of the midpoint for the clamped circular sandwich plate with an FGM central disk and two piezoelectric layers.

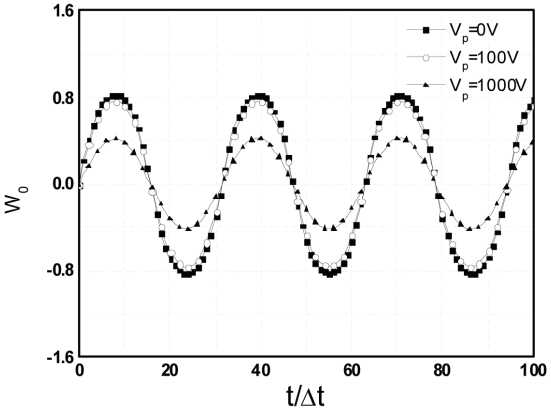


Fig. 9 The influence of the electrical excitation on the deflection distributions of midpoint for the clamped circular sandwich plate with an FGM central disk and two piezoelectric layers.

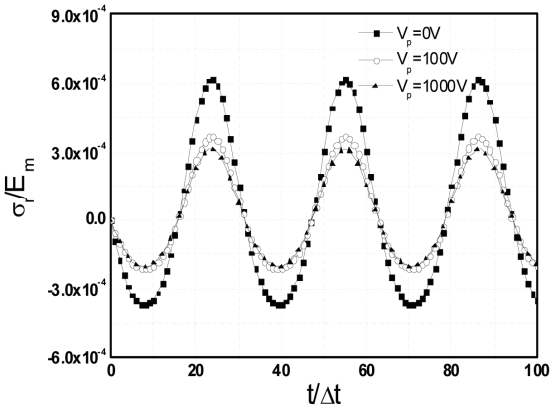


Fig. 10 The influence of the electrical excitation on the radial stress distributions for the clamped circular sandwich plate with an FGM central disk and two piezoelectric layers at $z = 0$ and $r = 1/2a$.

https://doi.org/10.1017/jmech.2015.7 Published online by Cambridge University Press

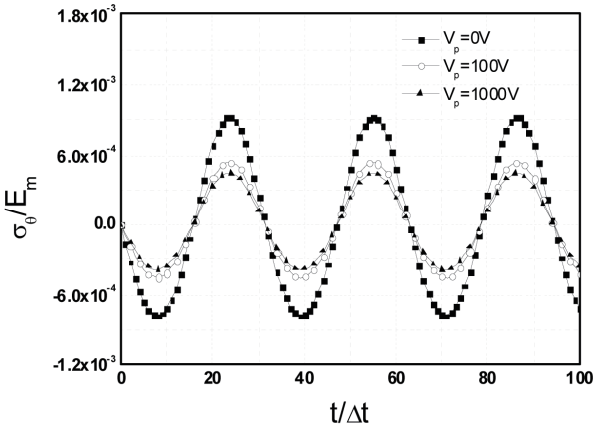


Fig. 11 The influence of the electrical excitation on the hoop stress distributions for the clamped circular sandwich plate with an FGM central disk and two piezoelectric layers at $z = 0$ and $r = 1/2a$.

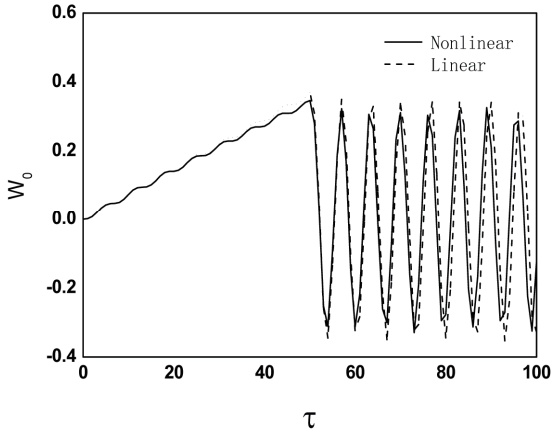


Fig. 12 Comparison of linear and nonlinear deflection distributions of the midpoint for the clamped circular sandwich plate with an FGM central disk and two piezoelectric layers.

the deflection and control the vibration of the circular sandwich plate through the design of the piezoelectric layer. From Figs. 10 and 11, it can be found that the distributions of radial and hoop stresses for the circular sandwich plate decrease as the electric excitation increases, and the amplitude of the hoop stress is always bigger than that of the radial stress at the same conditions.

Example 4. Considering a clamped circular sandwich plate with an FGM central disk and two piezoelectric layers subjected to impact load, and the impact load can be expressed as follows

$$q(t) = 5\times10^{8} t\,(Pa)\,,\ t \le 10^{-2}\,s \tag{23a}$$

$$q(t) = 0\,(Pa)\,,\ t > 10^{-2}\,s \tag{23b}$$

and other conditions are the same as the Example 2.

Figure 12 depicts the linear and nonlinear transient response of the midpoint deflection for the circular sandwich plate with an FGM central disk and two piezoelectric layers subjected to a suddenly impact load, where $a = 0.5$m, $h = 0.05$m, $H = 0.06$m and $n = 5$. From the figure, one finds, the greater impact load is, and the circular sandwich plate will be in the free vibration after the impact load reaching maximum value. It is also found from the figure that the amplitude of the free vibration is almost equal to the corresponding value as the pressure is abrupt dismissed. The result reveals that the linear dynamic response of the circular sandwich plate is bigger than that of the nonlinear analysis.

Figures 13 and 14 shows, respectively, the deflection distribution of the midpoint for the circular sandwich plate with different ratios of thickness to radius h/a and volume fraction indexes n. From two figures, it is found that the amplitude of the vibration during the loading time ($t < 0.01$s, that is, $t/\Delta t < 50$) are close to those after the time when the pressure is suddenly disappeared ($t \ge 0.01$s). It is noted from the Fig. 13 that the amplitude of the midpoint deflection for the circular

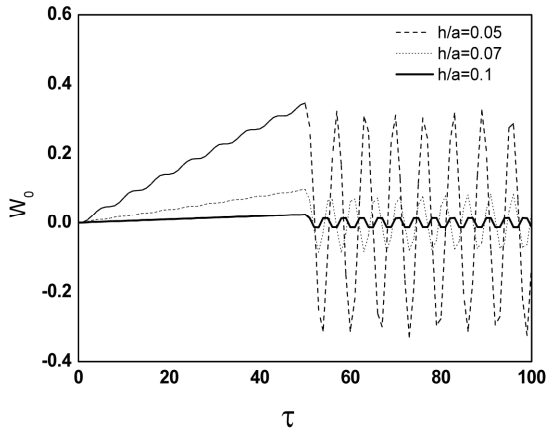


Fig. 13 The influence of the ratios of thickness to radius on the deflection distributions of the midpoint for the clamped circular sandwich plate with an FGM central disk and two piezoelectric layers.

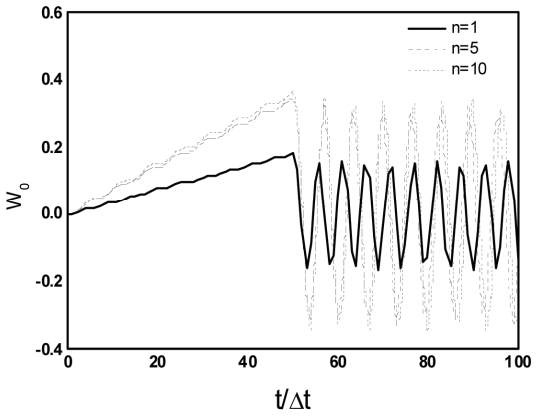


Fig. 14 The influence of the volume fraction index n on the deflection distributions of midpoint for the clamped circular sandwich plate with an FGM central disk and two piezoelectric layers.

https://doi.org/10.1017/jmech.2015.7 Published online by Cambridge University Press

sandwich plate decreases as the ratio of thickness to radius increases, in the other words, it takes a shorter time to suppress the vibration of a thick circular plate efficiently than that of a comparatively thin one. From the Fig. 14, It is seen that the amplitude of the midpoint deflection for the circular sandwich plate decreases as the volume fraction index n increases. It can be noticed that, when n is set a large value, high metal components and low Young's modulus of the FGM central disk for the circular sandwich plate can be observed. Hence, the bending stiffness of the circular sandwich plate reduces, and the amplitude and a low free vibration frequency for the circular sandwich plate under the impact load can be concluded.

5. CONCLUSIONS

Based on the Hamilton's variational principle, transient response analysis of the circular sandwich plate with an FGM central disk and two piezoelectric layers is presented by adopting the finite difference method, Newmark method and iterative method. Effect of material parameters, load parameters and geometric size on wave propagation of the deflection and stresses for the circular sandwich plate are discussed in detail and some useful conclusions have been drawn as follows.

1. Under a simple harmonic excitation, the bigger the ratio of thickness to radius, piezoelectric layer's thickness and electrical load is, the smaller the amplitudes of the midpoint deflection and stresses for the circular sandwich plate with an FGM central disk and two piezoelectric layers is, moreover, the amplitude of deflection and stresses decreases as the volume fraction index n increases.
2. Under an impact load, the initial deflection of the circular sandwich plate with an FGM central disk and two piezoelectric layers reaches maximum when the impact load is eliminated, and then it will be into the free vibration. Under the same impact load, geometrical nonlinearity and the increasing of the ratio of thickness to radius for the circular sandwich plate make the free vibration amplitude smaller and the free vibration frequency greater, however, the effect of the volume fraction indexes n is contrary.

ACKNOWLEDGEMENTS

The authors wish to thank reviewers for their valuable comments and the research is supported by the National Natural Science Foundation of China (11372105), New Century Excellent Talents Program in University (NCET-13-0184), Key Laboratory of Manufacture and Test Techniques for Automobile Parts (Chongqing University of Technology), Ministry of Education (2012KLMT01), Hunan Provincial Natural Science Foundation for Creative Research Groups of China (12JJ7001), and the central colleges of basic scientific research and operational costs (funded by the Hunan University).

REFERENCES

1. Koizumi, M., "Concept of FGM," *Ceramic Transactions*, **34**, pp. 3–10 (1993).
2. Chen, L. and Hirai, T., "Recent and Prospective Development of Functionally Graded Materials in Japan," *Materials Science Forum*, pp. 308–311 and pp. 509–514 (1999).
3. Hirai, T., "Functionally Gradient Materials and Nanocomposites," *American Ceramic Society*, **34**, pp. 11–20 (1993).
4. Paulino, G. H., Jin, Z. H. and Dodds, J. R. H., *Failure of Functionally Graded Materials*, Elsevier Science, New York (2003).
5. Zhang, W., Yang, J. and Hao, Y. X., "Chaotic Vibrations of an Orthotropic FGM Rectangular Plate Based on Third Shear Deformation Theory," *Nonlinear Dynamics*, **59**, pp. 619–660 (2010).
6. Yang, J., Hao, Y. X., Zhang, W. and Kitipornchai, S., "Nonlinear Dynamic Response of a Functionally Graded Plate with a Through-Width Surface Crack," *Nonlinear Dynamics*, **59**, pp. 207–219 (2010).
7. Ma, L. S. and Wang, T. J., "Relationships Between Axisymmetric Bending and Buckling Solutions of FGM Circular Plates Based on Third-Order Plate Theory and Classical Plate Theory," *International Journal of Solids and Structures*, **41**, pp. 85–101 (2004).
8. Li, S. R., Zhang, J. H. and Zhao, Y. G., "Nonlinear Thermomechanical Post-Buckling of Circular FGM Plate with Geometric Imperfection," *Thin-Walled Structures*, **45**, pp. 528–536 (2007).
9. Saidi, A. R., Rasouli, A. and Sahraee, S., "Axisymmetric Bending and Buckling Analysis of Thick Functionally Graded Circular Plates Using Unconstrained Third-Order Shear Deformation Plate Theory," *Composite Structures*, **89**, pp. 110–119 (2009).
10. Hosseini-Hashemi, S. H., Fadaee, M. and Eshaghi, M., "A Novel Approach for In-Plane/Out-Of-Plane Frequency Analysis of Functionally Graded Circular/Annular Plates," *International Journal of Mechanical Sciences*, **52**, pp. 1025–1035 (2010).
11. Alijani, F., Bakhtiari-Nejad, F. and Amabili, M., "Nonliear Vibrations of FGM Rectangular Plates in Thermal Environments," *Nonlinear Dynamics*, **66**, pp. 251–270 (2011).
12. Hu, Y. D. and Zhang, Z. Q., "The Bifurcation Analysis on the Circular Functionally Graded Plate with Combination Resonances," *Nonlinear Dynamics*, **67**, pp. 1779–1790 (2012).
13. Dai, H. L. and Zhen, H. Y., "Creep Buckling and Post-Buckling Analyses of a Viscoelastic FGM Cylindrical Shell with Initial Deflection Subjected to a Uniform In-Plane Load," *Journal of Mechanics*, **28**,

https://doi.org/10.1017/jmech.2015.7 Published online by Cambridge University Press

pp. 391–399 (2012).
14. Xie, H., Dai, H. L. and Rao, Y. N., "Thermoelastic Dynamic Behaviors of a FGM Hollow Cylinder Under Non-Axisymmetric Thermo-Mechanical Loads," *Journal of Mechanics*, **29**, pp. 109–120 (2013).
15. Dai, H. L., Yang, X. and Yang, L., "Nonlinear Dynamic Analysis for FGM Circular Plates," *Journal of Mechanics*, **29**, pp. 287–296 (2013).
16. Golmakani, M. E. and Kadkhodayan, M., "An Investigation Into the Thermoelastic Analysis of Circular and Annular Functionally Graded Material Plates," *Mechanics of Advanced Materials and Structures*, **21**, pp. 1–13 (2014).
17. Zhong, Z. and Shang, E. T., "Exact Analysis of Simply Supported Functionally Graded Piezothermoelectric Plates," *Journal of Intelligent Material Systems and Structures*, **16**, pp. 643–651 (2005).
18. Li, X. Y., Ding, H. J. and Chen, W. Q., "Three-Dimensional Analytical Solution for a Transversely Isotropic Functionally Graded Piezoelectric Circular Plate Subject to a Uniform Electric Potential Difference," *Science in China Series G: Physics, Mechanics and Astronomy*, **51**, pp. 1116–1125 (2008).
19. Birschetto, S. and Carrera, E., "Refined 2D Models for the Analysis of Functionally Graded Piezoelectric Plates," *Journal of Intelligent Material Systems and Structures*, **20**, pp. 1783–1797 (2009).
20. Wang, Y., Xu, R. Q. and Ding, H. J., "Analytical Solutions of Functionally Graded Piezoelectric Circular Plates Subjected to Axisymmetric Loads," *Acta Mechanica*, **215**, pp. 287–305 (2010).
21. Alibeigloo, A., "Thermo-Elasticity Solution of Functionally Graded Plates Integrated with Piezoelectric Sensor and Actuator Layers," *Journal of Thermal Stresses*, **33**, 754–774 (2010).
22. Mao, Y. Q., Fu, Y. M. and Dai, H. L., "Creep Buckling and Post-Buckling Analysis of the Laminated Piezoelectric Viscoelastic Functionally Graded Plates," *European Journal of Mechanics-A/Solids*, **30**, pp. 547–558 (2011).
23. Li, X. Y., Wu, J., Ding, H. J. and Chen, W. Q., "3D Analytical Solution for a Functionally Graded Transversely Isotropic Piezoelectric Circular Plate Under Tension and Bending," *International Journal of Engineering Science*, **49**, pp. 664–676 (2011).
24. Javanbakht, M., Shakeri, M., Sadeghi, S. N. and Daneshmehr, A. R., "The Analysis of Functionally Graded Shallow and Non-Shallow Shell Panels with Piezoelectric Layers Under Dynamic Load and Electrostatic Excitation Based on Elasticity," *European Journal of Mechanics-A/Solids*, **30**, pp. 983–991 (2011).
25. Birman, V., "Examples of Advanced Applications: Plates with Piezoelectric Sensors and Actuators and Functionally Graded Plates," *Plate Structures,* Springer Netherlands, **178**, pp. 257–293 (2011).
26. Khorshidvand, A. R., Jabbari, M. and Eslami, M. R., "Thermoelastic Buckling Analysis of Functionally Graded Circular Plates Integrated with Piezoelectric Layers," *Journal of Thermal Stresses*, **35**, pp. 695–717 (2012).
27. Sladek, J., Sladek, V., Stanak, P., Zhang, C. Z. and Wünsche, M., "Analysis of the Bending of Circular Piezoelectric Plates with Functionally Graded Material Properties by a MLPG Method," *Engineering Structures*, **47**, pp. 81–89 (2013).
28. Woo, J. and Meguid, S., "Nonlinear Analysis of Functionally Graded Plates and Shallow Shells," *International Journal of Solids and Structures*, **38**, pp. 7409–7421 (2001).
29. Ebrahimi, F., Rastgoo, A. and Kargarnovin, M., "Analytical Investigation on Axisymmetric Free Vibrations of Moderately Thick Circular Functionally Graded Plate Integrated with Piezoelectric Layers," *Journal of Mechanical Science and Technology*, **22**, pp. 1058–1072 (2008).
30. Najafizadeh, M. M. and Eslami, M. R., "Buckling Analysis of Circular Plates of Functionally Graded Materials Under Uniform Radial Compression," *International Journal of Mechanical Sciences*, **44**, pp. 2479–2493 (2002).
31. Timoshenko, S. and Goodier, J. N., *Theory of Elasticity*, McGraw-Hill, New York (1951).
32. Timoshenko, S. and Woinowsky-Krieger, S., *Theory of Plates and Shells*, McGraw-Hill, New York (1959).
33. Reddy, J. N. and Huang, C. L., "Nonlinear Axisymmetric Bending of Annular Plates with Varying Thickness," *International Journal of Solids and Structures*, **17**, pp. 811–825 (1981).
34. Reddy, J. N., Wang, C. M. and Kitipornchai, S., "Axisymmertric Bending of Functionally Graded Circular and Annular Platesm," *European Journal of Mechanics-A/Solids*, **18**, pp. 185–199 (1999).
35. Sahraee, S. and Saidi, A. R., "Axisymmertric Bending Analysis of Thick Functionally Graded Circular Plates Using Fourth-Order Shear Deformation Theory," *European Journal of Mechanics-A/Solids*, **28**, pp. 974–984 (2009).
36. Allahverdizadeh, A., Naei, M. and Nikkhah, B. M., "Vibration Amplitude and Thermal Effects on the Nonlinear Behavior of Thin Circular Functionally Graded Plates," *International Journal of Mechanical Sciences*, **50**, pp. 445–454 (2008).
37. Gautschi, W., *Numerical Analysis*, Springer, New York (2011).
38. Bodaghi, M., Damanpack, A. R., Aghdam, M. M. and Shakeri, M., "Non-Linear Active Control of FG Beams in Thermal Enviroments Subjected to Blast Loads with Integrated FGP Sensor/Actuator Layers," *Composite Structures*, **94**, pp. 3612–3623 (2012).

(Manuscript received May 9, 2014,
accepted for publication October 19, 2014.)

https://doi.org/10.1017/jmech.2015.7 Published online by Cambridge University Press